UNIVERSITAT POLITÈCNICA DE CATALUNYA

Power flow control of a doubly-fed induction machine coupled to a flywheel

Carles Batlle, Arnau Dòria-Cerezo, Romero Ortega

Institut d'Organització i Control de Sistemes Industrials

Power Flow Control of a Doubly–Fed Induction Machine Coupled to a Flywheel[*]

Carles Batlle[1,2][†], Arnau Dòria-Cerezo[2][‡] and Romeo Ortega[3]

[1] Department of Applied Mathematics IV, UPC
EPSEVG, Av. V. Balaguer s/n, 08800 Vilanova i la Geltrú, Spain.
[2] Institute of Industrial and Control Engineering, UPC
Av. Diagonal 647, 08028 Barcelona, Spain.
[3] Lab. des Signaux et Systèmes
CNRS-SUPELEC, Gif-sur-Yvette 91192, France.

Abstract

We consider a doubly–fed induction machine—controlled through the rotor voltage and connected to a variable local load—that acts as an energy–switching device between a local prime mover (a flywheel) and the electrical power network. The control objective is to optimally regulate the power flow which is achieved commuting between two different steady–state regimes. We first show that the zero dynamics of the system is only marginally stable complicating its control via feedback linearization. Instead, we apply the energy–based Interconnection and Damping Assignment Passivity–Based Control technique that does not require stable invertibility. It is shown that the partial differential equation that appears in this method can be obviated fixing the desired closed-loop total energy and adding new terms to the interconnection structure. Furthermore, to obtain a globally defined control law we introduce a state–dependent damping term that has the nice interpretation of effectively decoupling the electrical and mechanical parts of the system. This results in a globally asymptotically stabilizing controller parameterized by two degrees of freedom, which can be used to implement the power management policy. An indirect adaptive scheme for the rotor and stator resistances is also introduced. The controller is simulated and shown to work satisfactorily for various realistic load changes.

1   Introduction

Doubly–fed induction machines (DFIM) have been proposed in the literature, among other applications, for high performance storage systems [2], wind-turbine generators [13][14][16] or hybrid engines [3]. The attractiveness of the DFIM stems primarily from its ability to handle large speed variations around the synchronous speed (see [19] for an extended literature survey and discussion.) In this paper we are interested in the application of DFIM as part of an autonomous energy–switching system that regulates the energy flow between a local prime mover (a flywheel) and the electrical power network to satisfy the demand of a time–varying electrical load.

Most DFIM controllers proposed in the literature are based on vector–control and decoupling [9]. Along these lines, an output feedback algorithm for power control with rigorous stability and robustness results is presented in [19]. In this paper we propose an alternative viewpoint and use the energy–based principles of passivity and control as interconnection [4] [8] [11] [20]. More specifically, we prove that the Interconnection and Damping Assignment Passivity–Based Control (IDA–PBC) technique proposed in [11] can be easily applied to regulate the dynamic operation of this bidirectional power flow system.

The paper is organized as follows. In Section 2 we introduce the architecture of the system to be controlled and derive its model. Since IDA–PBC concerns the stabilization of equilibrium points, we use the Blondel–Park synchronous dq-coordinates[1] to write the equations in the required form. Then, to render more transparent the application of IDA–PBC, we give the Port–Controlled Hamiltonian (PCH) version of the model. Section 3 discusses the zero dynamics of interest for the kind of task we are trying to solve and show it to be only marginally stable—hampering the application of feedback linearization principles. The power management scheme consists of the assignment of suitable fixed points and is introduced in Section 4. The main result of the paper is a globally stable IDA–PBC controller that is presented in Section 5. We start with the solution of the partial differential equation (PDE) that arises in IDA–PBC by direct assignment of the desired energy function and modification of the interconnection structure. Unfortunately, the resulting control law contains a singularity, hence it is not globally defined. To remove this singularity we introduce a state–dependent damping that, in the spirit of the nested–loop PBC configuration of Chapter 8 in [10], has the nice interpretation of effectively decoupling the electrical and mechanical parts of the system. Section 6 introduces an indirect adaptive scheme to cope with some of the time–varying parameters of the DFIM and Section 7 presents the results of several simulations. Conclusions are stated in Section 8.

Notation   Throughout the paper we use standard notation of electromechanical systems, with $\lambda, v, i, \tau, \theta, \omega$ denoting flux, voltage, current, couple, angular position and velocity, respectively; while R, L, J, B are used for resistance, inductance, inertia and friction parameters, respectively. Self–explanatory sub–indices are introduced also for the signals and parameters of the different subsystems. Finally, to underscore the port interconnection structure of the overall system we usually present the variables in power conjugated couples, i.e., port variables whose product has units of power.

---

[1]In this coordinates the natural steady–state orbits are transformed into fixed points.
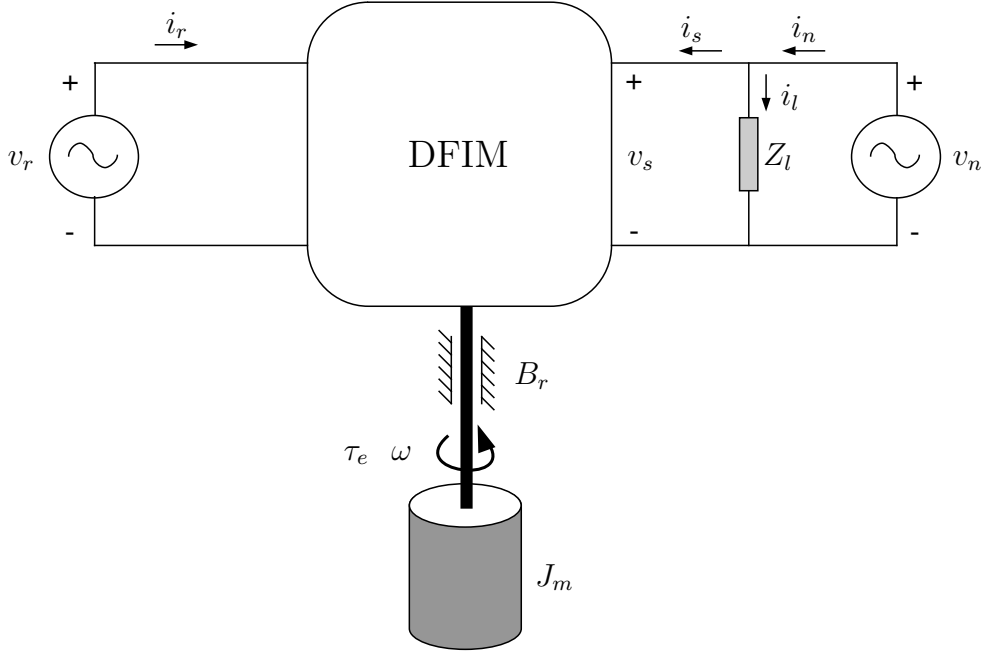
Figure 1: Doubly fed induction machine, flywheel, power network and load.

2   The System and its Mathematical Model

Figure 1 shows a DFIM, controlled through the rotor windings port (v_r, i_r), coupled to an energy–storing flywheel with port variables (τ_e, ω), an electrical network modelled by an ideal AC voltage source with port variables (v_n, i_n), and a generic electrical load represented by its impedance Z_l. Network equations are given by Kirchhoff laws

$$i_l = i_n - i_s, \quad v_n = v_s. \tag{1}$$

Figure 2 shows a scheme of a doubly-fed, three-phase induction machine. It contains 6 energy storage elements with their associated dissipations and 6 ports (the 3 stator and the 3 rotor voltages and currents).

From the original three phase electrical variables y_{abc} (currents, voltages or magnetic fluxes) we compute transformed variables by means of

$$y = T y_{abc}$$

where

$$T = \begin{pmatrix} \frac{\sqrt{2}}{\sqrt{3}} & -\frac{1}{\sqrt{6}} & -\frac{1}{\sqrt{6}} \\ 0 & \frac{1}{\sqrt{2}} & -\frac{1}{\sqrt{2}} \\ \frac{1}{\sqrt{3}} & \frac{1}{\sqrt{3}} & \frac{1}{\sqrt{3}} \end{pmatrix}.$$

Notice that, since $T^T = T^{-1}$, this is a power–preserving transformation:

$$\langle i, v \rangle = \langle i_{abc}, v_{abc} \rangle.$$

As it is common, from now on we will work only with the two first components (the dq components) of any electrical quantity and neglect the third one (the homopolar
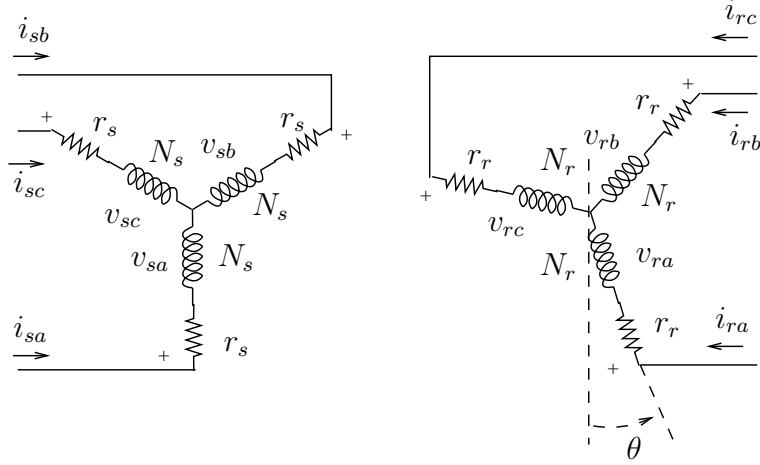
Figure 2: Basic scheme of the doubly fed induction machine

component, which is zero for any balanced set and which, in any case, is decoupled from the remaining dynamical equations.)

The electrical equations of motion in the original windings frame for the dq variables, neglecting nonlinear effects and non–sinusoidal magnetomotive force distribution, take the form [6] [7],

$$\dot{\lambda}_s + R_s i_s = v_s \tag{2}$$

$$\dot{\lambda}_r + R_r i_r = v_r \tag{3}$$

where $\lambda_s, \lambda_r, i_s, i_r \in \mathbb{R}^2$ and $R_s = \text{diag}(r_s, r_s) > 0$, $R_r = \text{diag}(r_r, r_r) > 0$, while the mechanical equations are given by (we assume without loss of generality a 2-poles machine)

$$J_m \dot{\omega} = L_{sr} i_s^T J_2 i_r - B_r \omega \tag{4}$$

$$\dot{\theta} = \omega$$

where $\theta \in \mathbb{R}$, $J_m > 0$, $B_r \geq 0$, $L_{sr} > 0$ and we defined

$$J_2 = \begin{pmatrix} 0 & -1 \\ 1 & 0 \end{pmatrix}.$$

Linking fluxes and currents are related by

$$\lambda = L(\theta)i$$

where

$$\lambda = \begin{bmatrix} \lambda_s \\ \lambda_r \end{bmatrix}, \quad i = \begin{bmatrix} i_s \\ i_r \end{bmatrix}, \quad L(\theta) = \begin{bmatrix} L_s I_2 & L_{sr} e^{J_2 \theta} \\ L_{sr} e^{-J_2 \theta} & L_r I_2 \end{bmatrix}, \quad I_2 = \begin{bmatrix} 1 & 0 \\ 0 & 1 \end{bmatrix},$$

with $L_s, L_r > 0$ and $L_s L_r > L_{sr}^2$. Putting together (2) and (3) we get

$$\dot{\lambda} + \mathcal{R}i = V$$

where

$$V = \begin{bmatrix} v_s \\ v_r \end{bmatrix}, \quad \mathcal{R} = \begin{bmatrix} R_s I_2 & O_2 \\ O_2 & R_r I_2 \end{bmatrix}, \quad O_2 = \begin{bmatrix} 0 & 0 \\ 0 & 0 \end{bmatrix}$$

The steady–state for the equations above are periodic orbits that can be transformed into equilibrium points by means of the so-called Blondel-Park transformation. This standard procedure also eliminates the dependence of the equations on θ, and consists in defining new variables f^r via

$$f = K(\theta, \delta) f^r$$

$$K(\theta, \delta) = \begin{bmatrix} e^{J_2\delta} & O_2 \\ O_2 & e^{J_2(\delta-\theta)} \end{bmatrix}$$

where δ is an arbitrary function of time that, for convenience, we select as

$$\dot{\delta} = \omega_s,$$

with ω_s the line frequency, which is assumed constant.[2]

Applying this transformation to all the electrical variables, one gets

$$\mathcal{L}\dot{x} + [\Omega(\omega)\mathcal{L} + \mathcal{R}]x = M_1 u + M_2 v_s^r \tag{5}$$

where

$$x = \begin{bmatrix} i_s^r \\ i_r^r \end{bmatrix}, \quad u = v_r^r, \quad v_s^r = \begin{bmatrix} V_0 \\ 0 \end{bmatrix}$$

$$\mathcal{L} = K^{-1}(\theta, \delta) L(\theta) K(\theta, \delta) = \begin{bmatrix} L_s I_2 & L_{sr} I_2 \\ L_{sr} I_2 & L_r I_2 \end{bmatrix}$$

$$\Omega(\omega)\mathcal{L} = \begin{bmatrix} \omega_s L_s J_2 & \omega_s L_{sr} J_2 \\ (\omega_s - \omega) L_{sr} J_2 & (\omega_s - \omega) L_r J_2 \end{bmatrix}$$

$$M_1 = \begin{bmatrix} O_2 \\ I_2 \end{bmatrix}, \quad M_2 = \begin{bmatrix} I_2 \\ O_2 \end{bmatrix}$$

with $V_0 > 0$ the constant voltage set by the power network.

Summarizing: the overall system consists of the fourth–order electrical dynamics (5) together with the scalar mechanical dynamics (4). The control input is the two–dimensional rotor voltage u, and v_s^r is viewed as a constant disturbance.[3]

As discussed in [4] (and references therein) a large class of physical systems of interest in control applications can be modelled in the general form of PCH systems[4]

$$\dot{z} = [\mathcal{J}(z) - \mathcal{R}(z)](\nabla H)^T + g(z)u$$

where z is the state, $H(z)$ is the total energy of the system (representing its energy), $\mathcal{J}(z) = -\mathcal{J}^T(z)$ is the interconnection matrix and $\mathcal{R}_d(z) = \mathcal{R}^T(z) \geq 0$ the dissipation matrix. It is easy to see that PCH systems are passive with port variables $(u, g^T(z)(\nabla H)^T)$ and storage function the total energy. Before closing this section we derive the PCH model of the system, a step which is instrumental for the application of the IDA–PBC methodology.

---

[2] This is the so–called synchronous reference frame. Notice the simple form of v_s^r in this frame.

[3] To simplify the notation, in the sequel we will omit the super–index $(\cdot)^r$.

[4] To distinguish between energy–conserving and dissipating systems the latter are sometimes called PCHD systems.

To cast our system into this framework it is convenient to select as state coordinates the natural electromechanical Hamiltonian variables, fluxes (λ) and (angular) momentum ($J_m\omega$), that is

$$z = \begin{bmatrix} z_e \\ z_m \end{bmatrix} = \begin{bmatrix} \lambda \\ J_m\omega \end{bmatrix},$$

where, for convenience, we have introduced a natural partition between electrical ($z_e \in \mathbb{R}^4$) and mechanical ($z_m \in \mathbb{R}$) coordinates. The equations of our system can be written as [15]

$$\dot{z} = [\mathcal{J}(z) - \mathcal{R}] (\nabla H)^T + B_1 v_r + B_2 v_s \tag{6}$$

with total energy

$$H(z) = \frac{1}{2} z_e^T \mathcal{L}^{-1} z_e + \frac{1}{2J_m} z_m^2,$$

interconnection and dissipation matrices

$$\mathcal{J}(z) = \begin{bmatrix} -\omega_s L_s J_2 & -\omega_s L_{sr} J_2 & O_{2\times 1} \\ -\omega_s L_{sr} J_2 & -(\omega_s - \omega) L_r J_2 & L_{sr} J_2 i_s \\ O_{1\times 2} & L_{sr} i_s^T J_2 & 0 \end{bmatrix}, \quad \mathcal{R} = \begin{bmatrix} R_s I_2 & O_2 & O_{2\times 1} \\ O_2 & R_r I_2 & O_{2\times 1} \\ O_{1\times 2} & O_{1\times 2} & B_r \end{bmatrix},$$

respectively, and

$$B_1 = \begin{bmatrix} O_2 \\ I_2 \\ O_{2\times 1} \end{bmatrix}, \quad B_2 = \begin{bmatrix} I_2 \\ O_2 \\ O_{2\times 1} \end{bmatrix}.$$

Notice that the gradient of the Hamiltonian yields the original, Lagrangian (or co-energy) variables:

$$(\nabla H)^T = \begin{bmatrix} \mathcal{L}^{-1} z_e \\ \frac{1}{J_m} z_m \end{bmatrix} = \begin{bmatrix} x \\ \omega \end{bmatrix}$$

3 Zero Dynamics

We will study the zero dynamics of the system, taking as output the stator current, *i.e.*,

$$y = Cx$$

where $C = \begin{bmatrix} I_2 & O_2 \end{bmatrix}$. One easily gets

$$\dot{y} = C\mathcal{L}^{-1}[-(\Omega(\omega)\mathcal{L} + \mathcal{R})x + M_1 u + M_2 v_s].$$

Consistent with the problem formulation (that is given in Section 4) we consider a constant desired output of the form $y^* = i_s^*$, hence $\dot{y}^* = 0$ and the decoupling and linearizing control is given by

$$u = D^{-1} C\mathcal{L}^{-1}[(\Omega(\omega)\mathcal{L} + \mathcal{R})x - C\mathcal{L}^{-1} M_2 v_s]$$

with

$$D = C\mathcal{L}^{-1} M_1 = -\frac{L_{sr}}{L_s L_r - L_{sr}^2} I_2 < 0,$$

where negative definiteness stems from the fact that $L_s L_r > L_{sr}^2$. Substituting this control into the system equations, one gets the following dynamics

$$\dot{x} = \mathcal{A}x - \mathcal{L}^{-1}(I_4 - M_1 D^{-1} C \mathcal{L}^{-1}) M_2 v_s$$

with

$$\mathcal{A} = -\mathcal{L}^{-1}[\Omega(\omega)\mathcal{L} + \mathcal{R} - M_1 D^{-1} C \mathcal{L}^{-1}(\Omega(\omega)\mathcal{L} + \mathcal{R})].$$

Some lengthy, but straightforward, calculations yield

$$\mathcal{A} = \begin{bmatrix} 0 & 0 \\ -\frac{1}{L_{sr}}(\omega_s L_s J_2 + R_s I_2) & -\omega_s J_2 \end{bmatrix}$$

which, interestingly, is a constant matrix independent of ω, with the forcing term matrix

$$\mathcal{L}^{-1}(I_4 - M_1 D^{-1} C \mathcal{L}^{-1}) M_2 = \begin{bmatrix} 0 \\ 0 \\ * \\ * \end{bmatrix}$$

where $*$ denotes some non–zero constants. Consequently, the zero dynamics is a linear oscillator with a constant forcing input that depends on v_s. It is well–known that a linear oscillator is not bounded–input bounded–output stable hence unbounded trajectories of the forced system may appear upon change of the line voltage, which stymies the control of the system by direct inversion.

We should underscore that a similar result is obtained if we take as output the rotor, instead of the stator, current [18].

4 Power Flow Strategy

The power management schedule is determined according to the following considerations. The general goal is to supply the required power to the load with a high network power factor, $i.e.$, $Q_n \sim 0$, where Q_n is the network reactive power. On the other hand, we will show below that the DFIM has an optimal mechanical speed for which there is minimal power injection through the rotor. Combining these two factors suggests to consider the following three modes of operation:

- (Generator mode) When the real power required by the local load is bigger than the maximum network power (say, P_n^M) we use the machine as a generator. In this case we fix the references for the network real and reactive powers as $P_n^* = P_n^M$ and $Q_n^* = 0$.

- (Storage mode) When the local load does not need all the network power and the mechanical speed is far from the optimal value the "unused" power network is employed to accelerate the flywheel. From the control point of view, this operation mode is the same that the generator mode thus we fix the same references—but now we want to extract the maximum power from the network to transfer it to the flywheel.

– *(Stand-by mode)* Finally, when the local load does not need all the power network and the mechanical speed is near to the optimal one we just compensate for the flywheel friction losses by regulating the speed and the reactive power. Henceforth, we fix the reference for the mechanical speed at its minimum rotor losses value (to be defined below) and set $Q_n^* = 0$.

The operation modes boil down to two kinds of control actions (we call them 0 and 1) as expressed in Table 1, where $\epsilon > 0$ is some small parameter.

$P_n^* < P_l$	$|\omega - \omega_s| \leq \epsilon$	Mode	Control	References
True	True	Generator	0	$P_n^* = P_n^M$ and $Q_n^* = 0$
True	False	Generator	0	$P_n^* = P_n^M$ and $Q_n^* = 0$
False	True	Storage	0	$P_n^* = P_n^M$ and $Q_n^* = 0$
False	False	Stand-by	1	$Q_n^* = 0$ and $\omega^* = \omega_s$

Table 1: Control action table.

The formulate mathematically the power flow strategy described above we need to express the various modes in terms of equilibrium points. In this way, the policy will be implemented transferring the system from one equilibrium point to another. Towards this end, we compute first the fixed points of our system, *i.e.* the values $z_e^* = \mathcal{L}i^*$, $z_m^* = J_m\omega^*$, v_r^* such that

$$[\mathcal{J}(z^*) - \mathcal{R}] \begin{bmatrix} i^* \\ \omega^* \end{bmatrix} + B_1 v_r^* + B_2 v_s = 0.$$

Explicit separation of the rows corresponding to the stator, rotor, network and mechanical equations yields the following system:

$$\omega_s L_s J_2 i_s^* + \omega_s L_{sr} J_2 i_r^* + R_s i_s^* - v_s = 0 \tag{7}$$

$$(\omega_s - \omega^*)[L_{sr} J_2 i_s^* + L_r J_2 i_r^*] + R_r i_r^* - v_r^* = 0 \tag{8}$$

$$L_{sr} i_s^{*T} J_2 i_r^* - B_r \omega^* = 0. \tag{9}$$

It is clear that—assuming no constraint on v_r—the key equations to be solved are (7) and (9).

As discussed above, a DFIM has an optimal mechanical speed for which there is minimal power injection through the rotor. Indeed, from (8) one immediately gets

$$P_r \equiv i_r^{*T} v_r^* = (\omega_s - \omega^*) L_{sr} i_r^{*T} J_2 i_s^* + R_r |i_r^*|^2,$$

where $|\cdot|$ is the Euclidean norm. Further, using (9), we get

$$P_r = B_r \omega^* (\omega^* - \omega_s) + R_r |i_r^*|^2. \tag{10}$$

Although the ohmic term in (10) does depend also on ω, its contribution is small for the usual range of parameter values, so $|P_r|$ is small near $\omega^* = \omega_s$. Another consideration that we make to justify our choice of "optimal" ω^* concerns the reactive power supplied to the rotor—that we would like to minimize. It can be shown that

$$Q_r \equiv i_r^{*T} J_2 v_r^* = (\omega^* - \omega_s) f(Q_n, \omega^*),$$

where f is a bounded function. Consequently, $Q_r = 0$ for $\omega^* = \omega_s$. Taking this into account, we will set the reference of the mechanical speed as $\omega^* = \omega_s$.

Let us explain now the calculations needed to determine the desired equilibria for the generating and stand–by modes. For, we recall that, assuming a sinusoidal steady–state regime, the network active and reactive powers are defined as

$$P_n \equiv i_n^T v_s = V_0 i_{nd} \tag{11}$$

$$Q_n \equiv i_n^T J_2 v_s = V_0 i_{nq}, \tag{12}$$

where we have denoted $i_n = [i_{nd}, i_{nq}]^T$.

In generating (and storage) mode we fix $P_n^* = P_n^M$ and $Q_n^* = 0$ thus immediately obtain from (11) and (12) that $i_n^* = [\frac{P_n^M}{V_0}, 0]^T$. Next, from equation (1) and the measured i_l we obtain i_s^* which, upon replacement on (7) yields i_r^*. Then, ω^* is computed from (9), and finally v_r^* is obtained via (8).

For the stand–by mode we still set $Q_n^* = 0$, but now fix $\omega^* = \omega_s$. This is a more complicated scenario as we have to ensure the existence of i_s^* and i_r^* solutions for the nonlinear equations (7) and (9). First of all, multiplying equation (7) by i_s^{*T} and using equation (9) one gets

$$R_s|i_s^*|^2 - v_s^T i_s^* + B_r \omega_s^2 = 0. \tag{13}$$

This is a quadratic equation that has an infinite number, a unique, or no solutions depending on whether ω_s is smaller, equal or larger than $\frac{V_0}{\sqrt{2B_r R_s}}$, respectively. Since B_r is usually a small coefficient typically there will be an infinite number of i_s^* that solve the equation. We will choose then the one of minimum norm. Once we have fixed i_s^* we can proceed as in the generating mode to compute i_r^* and v_r^*.

Before closing this section we make the interesting observation that, under the assumptions that the load can be modelled as a linear RL circuit and small friction coefficient, we can get a simple condition on the load parameters that ensure the existence of ω^* and P_n^*, with $Q_n^* = 0$. Indeed, tacking a general RL-load

$$Z_l = R_l I_2 + \omega_s L_l J_2,$$

replacing in (13), using (1), and the network power definitions (11), (12) we obtain

$$(P_n^*)^2 - |v_s|^2 \left(\frac{2R_l}{|Z_l|^2} + \frac{1}{R_s} \right) P_n^* + \frac{|v_s|^4}{|z_l|^2} \left(1 + \frac{R_l}{R_s} + \frac{2\omega_s L_l Q_n^*}{|v_s|^2} \right) - \frac{|v_s|^2 B_r \omega_s^2}{R_s} = 0.$$

In our case $Q_n^* = 0$ and considering $B_r = 0$ yields the quadratic equation

$$(P_n^*)^2 - |v_s|^2 \left(\frac{2R_l}{|Z_l|^2} + \frac{1}{R_s} \right) P_n^* + \frac{|v_s|^4}{|Z_l|^2} \left(1 + \frac{R_l}{R_s} \right) = 0.$$

It is easy to show that this equation has a positive real solution if and only if

$$R_s < \frac{R_l^2}{2\omega_s L_l} + \frac{\omega_s L_l}{2}, \tag{14}$$

hence it always has a real real solution for pure resistive loads, but the condition (14) appears when an RL load is connected.

5 Controller Design

As mentioned in the Introduction, to implement the proposed power flow strategy we design an IDA–PBC [11]. The central idea of this technique is to, still preserving the PCH structure, assign to the closed loop a desired energy function via the modification of the interconnection and dissipation matrices. That is, the desired target dynamics is a PCH system of the form

$$\dot{z} = [\mathcal{J}_d(z) - \mathcal{R}_d(z)](\nabla H_d)^T \tag{15}$$

where $H_d(z)$ is the new total energy and $\mathcal{J}_d(z) = -\mathcal{J}_d^T(z)$, $\mathcal{R}_d(z) = \mathcal{R}_d^T(z) > 0$, are the new interconnection and damping matrices, respectively. To achieve stabilization of the desired equilibrium point we impose

$$z^* = \arg\min H_d(z).$$

It is easy to see that the matching objective is achieved if and only if the following PDE is satisfied

$$[\mathcal{J}_d(z) - \mathcal{R}_d(z)](\nabla H_a)^T = -[\mathcal{J}_a(z) - \mathcal{R}_a(z)](\nabla H)^T + B_1 v_r + B_2 v_s. \tag{16}$$

where, for convenience, we have defined

$$H_d(z) = H(z) + H_a(z), \ \mathcal{J}_d(z) = \mathcal{J}(z) + \mathcal{J}_a(z), \ \mathcal{R}_d(z) = \mathcal{R}(z) + \mathcal{R}_a(z).$$

The standard way to solve (16) is to fix the matrices $\mathcal{J}_a(z)$ and $\mathcal{R}_a(z)$—hence the name IDA—and then solve the PDE for $H_a(z)$. In general, solving the PDE is a very complicated task. Fortunately, the special structure of our system allows us, in the spirit of [5, 15], to fix a quadratic $H_d(z)$ and then solve (16) for $\mathcal{J}_a(z)$ and $\mathcal{R}_a(z)$. Notice that v_s is fixed, so the only available control is in fact v_r.

5.1 Control Law

Following the strategy outlined above to solve the PDE (16), we choose the following desired total energy

$$H_d(z) = \frac{1}{2}(z_e - z_e^*)^T \mathcal{L}^{-1}(z_e - z_e^*) + \frac{1}{2J_m}(z_m - z_m^*)^2,$$

which clearly has a global minimum at the desired fixed point. This implies

$$H_a(z) = H_d(z) - H(z) = -z_e^{*T}\mathcal{L}^{-1}z_e - \frac{1}{J_m}z_m^*z_m + \frac{1}{2}z_e^{*T}\mathcal{L}^{-1}z_e^* + \frac{1}{2J_m}z_m^{*2}.$$

Notice that

$$(\nabla H_a)^T = \begin{bmatrix} -i^* \\ -\omega^* \end{bmatrix}.$$

Using this relation, (16) becomes

$$[\mathcal{J}_d(z) - \mathcal{R}_d(z)]\begin{bmatrix} i^* \\ \omega^* \end{bmatrix} = [\mathcal{J}_a(z) - \mathcal{R}_a(z)]\begin{bmatrix} i \\ \omega \end{bmatrix} - B_1 v_r - B_2 v_s. \tag{17}$$

The control action appears on the third and fourth rows, which suggests the choice

$$
\mathcal{J}_a(z) = \begin{bmatrix} O_2 & O_2 & O_{2\times 1} \\ O_2 & O_2 & -\mathcal{J}_{rm}(z) \\ O_{1\times 2} & \mathcal{J}_{rm}^T(z) & 0 \end{bmatrix}, \quad \mathcal{R}_a = \begin{bmatrix} O_2 & O_2 & O_{2\times 1} \\ O_2 & rI_2 & O_{2\times 1} \\ O_{1\times 2} & O_{1\times 2} & 0 \end{bmatrix} \quad (18)
$$

where $\mathcal{J}_{rm}(z) \in \mathbb{R}^{2\times 1}$ is to be determined, and we have injected an additional resistor $r > 0$ for the rotor currents to damp the oscillations in the tracking dynamics.

Substituting in (17) and using the fixed-point equations, one gets, after some algebra,

$$
\begin{aligned}
\mathcal{J}_{rm}^T(z) &= L_{sr} \frac{(i_r - i_r^*)^T}{|i_r - i_r^*|^2} (i_s - i_s^*)^T J_2 i_r^*, \\
v_r &= v_r^* - (\omega - \omega^*)(L_r J_2 i_r^* + \mathcal{J}_{rm}(z)) - L_{sr}\omega^* J_2(i_s - i_s^*) - rI_2(i_r - i_r^*).
\end{aligned}
$$

Unfortunately, the control is singular at the fixed point. Although from a numerical point of view we could implement it by introducing a regularization parameter, we are going to show below that it is possible to get rid of the singularity by adding a variable damping which turns out to decouple the mechanical and electrical subsystems.

5.2   Subsystem Decoupling via State–Dependent Damping

We keep the same $H_d(z)$ and $\mathcal{J}_d(z)$, but instead of the constant $\mathcal{R}_a$ given in (18) we introduce a state–dependent damping matrix

$$
\mathcal{R}_a(z) = \begin{bmatrix} O_2 & O_2 & O_{2\times 1} \\ O_2 & rI_2 & O_{2\times 1} \\ O_{1\times 2} & O_{1\times 2} & \xi(z) \end{bmatrix},
$$

where we set

$$
\xi(z) = \frac{\tau_e^* - \tau_e(z_e)}{\omega - \omega^*}
$$

with τ_e the electrical torque

$$
\tau_e = L_{sr} i_s^T J_2 i_r
$$

and $\tau_e^* = B_r \omega^*$ its fixed point value. Notice that, when substituted into the closed-loop Hamiltonian equations, $\xi(z)$ is multiplied by $\omega - \omega^*$ and hence no singularity is brought into the equations.

Since we only have changed the mechanical part of (17), only the value for $\mathcal{J}_{rm}(z)$ is changed while the expression for v_r in terms of $\mathcal{J}_{rm}(z)$ remains the same. After some algebra and using the fixed point equations, one gets

$$
\mathcal{J}_{rm}(z) = L_{sr} J_2 i_s.
$$

The closed loop dynamical system is still of the form (15) with

$$
\mathcal{J}_d(z) = \begin{bmatrix} -\omega_s L_s J_2 & -\omega_s L_{sr} J_2 & O_{2\times 1} \\ -\omega_s L_{sr} J_2 & -(\omega_s - \omega) L_r J_2 & O_{2\times 1} \\ O_{1\times 2} & O_{1\times 2} & 0 \end{bmatrix}, \mathcal{R}_d(z) = \begin{bmatrix} R_s I_2 & O_2 & O_{2\times 1} \\ O_2 & (R_r + r)I_2 & O_{2\times 1} \\ O_{1\times 2} & O_{1\times 2} & B_r + \xi(z) \end{bmatrix}.
$$

We underscore the fact that the main effect of the proposed control is to decouple the electrical and mechanical parts in the closed-loop interconnection and dissipation matrices.

5.3 Main Stability Result

Due to the fact that we cannot show that $B_r + \xi(z) > 0$, we cannot apply the standard stability analysis for PCH systems [20]. However, the overall system has a nice cascaded structure, with the electrical part a *bona fide* PCH subsystem with well–defined dissipation. (This situation is similar to the Nested PBC proposed in Chapter 8 of [10].) Asymptotic stability of the overall system follows from well known properties of cascaded systems [17]. For the sake of completeness we give the specific result required in our example in the form of a lemma in the Appendix.

We are in position to present the following:

Proposition 1 *Consider the DFIM system (6) in closed–loop with the static state–feedback control*

$$v_r = v_r^* - (\omega - \omega^*)(L_r J_2 i_r^* + L_{sr} J_2 i_s) - L_{sr}\omega^* J_2(i_s - i_s^*) - rI_2(i_r - i_r^*). \qquad (19)$$

Assume the motor friction coefficient B_m is sufficiently small to ensure the solution of the equilibrium equations (7) and (9) and v_r^* is given by (8). Then, each operating mode of the proposed power flow policy is globally asymptotically stable.

Proof. The proof follows immediately checking that the conditions of Lemma 1 in Appendix A. To do that, we identify x_1 with the electric variables and x_2 with the mechanical variable. The electric subsystem has (i_s^*, i_r^*) as a global asymptotically stable fixed point for any function $\omega(t)$. Hence the closed loop dynamics has (i_s^*, i_r^*, ω^*) as a global asymptotically stable point. ◁

6 Indirect adaptive scheme

In this section we present an indirect adaptive method (see [12] and references therein) to cope with the uncertainty of the machines resistances R_s and R_r. The method works for uncertain parameters appearing linearly in the dynamical equations, and could be extended to other system parameters.

Consider a system which can be expressed as

$$\dot{x} = f(x) + \Psi_s(x)\theta_s + \Psi_r(x)\theta_r + g(x)u$$

where θ_s and θ_r are the uncertain parameters. In our case, $\theta_s = R_s$, $\theta_r = R_r$, $x = z$,

$$f(x) + g(x)u = [\mathcal{J}(x) - \mathcal{R}'](\nabla H)^T + B_1 v_r + B_2 v_s,$$

and

$$\Psi_s(x) = -K_s(\nabla H)^T$$
$$\Psi_r(x) = -K_r(\nabla H)^T$$

with

$$K_s = \begin{bmatrix} I_2 & O_2 & O_{2\times1} \\ O_2 & O_2 & O_{2\times1} \\ O_{1\times2} & O_{1\times2} & 0 \end{bmatrix}, \quad K_r = \begin{bmatrix} O_2 & O_2 & O_{2\times1} \\ O_2 & I_2 & O_{2\times1} \\ O_{1\times2} & O_{1\times2} & 0 \end{bmatrix}, \quad \mathcal{R}' = \begin{bmatrix} O_2 & O_2 & O_{2\times1} \\ O_2 & O_2 & O_{2\times1} \\ O_{1\times2} & O_{1\times2} & B_r \end{bmatrix}.$$

We define $e = \hat{x} - x$, $\tilde{\theta}_s = \hat{\theta}_s - \theta_s$ and $\tilde{\theta}_r = \hat{\theta}_r - \theta_r$, where $\hat{x}$ obeys

$$\dot{\hat{x}} = f(x) + g(x)u + \Psi_s(x)\hat{\theta}_s + \Psi_r(x)\hat{\theta}_r - \Lambda e. \tag{20}$$

Then it is easy to show that

$$\dot{e} = \Psi_s(x)\tilde{\theta}_s + \Psi_r(x)\tilde{\theta}_r - \Lambda e.$$

The candidate Lyapunov function

$$V = \frac{1}{2}|e|^2 + \frac{1}{2\gamma_s}\tilde{\theta}_s^2 + \frac{1}{2\gamma_r}\tilde{\theta}_r^2$$

has derivative

$$\dot{V} = -e^T\Lambda e + e^T\Psi_s(x)\tilde{\theta}_s + \frac{1}{\gamma_s}\tilde{\theta}_s\dot{\tilde{\theta}}_s + e^T\Psi_r(x)\tilde{\theta}_r + \frac{1}{\gamma_r}\tilde{\theta}_r\dot{\tilde{\theta}}_r.$$

Then, to ensure $\dot{V} \leq 0$, we set

$$\dot{\tilde{\theta}}_s = \dot{\hat{\theta}}_s = -\gamma_s e^T\Psi_s(x). \tag{21}$$

$$\dot{\tilde{\theta}}_r = \dot{\hat{\theta}}_r = -\gamma_r e^T\Psi_r(x). \tag{22}$$

Equations (20), (21) and (22) define the identifier. A certainly equivalent control is obtained replacing the actual parameters by their estimator in (19).

7 Simulations

In this Section we implement a numerical simulation of the IDA–PBC Hamiltonian scheme developed in the previous Sections. We use the following parameter values (in SI units): $L_{sr} = 0.041$, $L_r = L_s = 0.041961$, $J_m = 5.001$, $B_r = 0.005$. The machine ohmic resistances start at $R_s = 0.087$ and $R_r = 0.0228$, and are increased by 50% to simulate temperature effects.

We have simulated two varying loads, one resistive and the other resistive-inductive. The resistive load is initially $R_l = 1000$, changes to $R_l = 5$ at $t = 1$ in 0.2 seconds and returns to $R_l = 1000$ at $t = 1.8$ also in 0.2 seconds. The same envelope (shifted 4 s forward) is used for the second load, with values $R_l = 1000$, $L_l = 0.01$ and $R_l = 1$, $L_l = 0.01$. The voltage source is, in dq coordinates, $v_g = (380, 0)$. The simulation has been performed using the 20-sim [1] modelling and simulation software.

For the purposes of testing the controller, we have set a maximum power network $P_n = 10000$. The parameters of the adaptive scheme are $\Lambda = 10$, $\gamma_s = 5$ and $\gamma_r = 1$. The damping parameter is fixed at $r = 100000$. A hysteresis filter is used to prevent chattering around $\omega = \omega_s$.

Figure 3 shows the load and the network active power for a purely resistive load for $t \in [0, 4]$. Notice that P_n is never bigger than its maximum value even if the load demand is higher. After the load demand returns to its initial value, P_n is kept at its peak value to accelerate the flywheel, until it reaches the optimum speed. The evolution of ω during this sequence is also shown in Figure 3; the minimum attained represents 96% of the optimal speed ω_s.

Figure 4 corresponds to the varying resistive-inductive load for $t \in [4, 8]$; the reactive powers are also shown in this case. One should notice that, in spite of the huge change of reactive power by the load, Q_n is kept to zero. Also, the minimum mechanical speed is 99% of the optimal value.
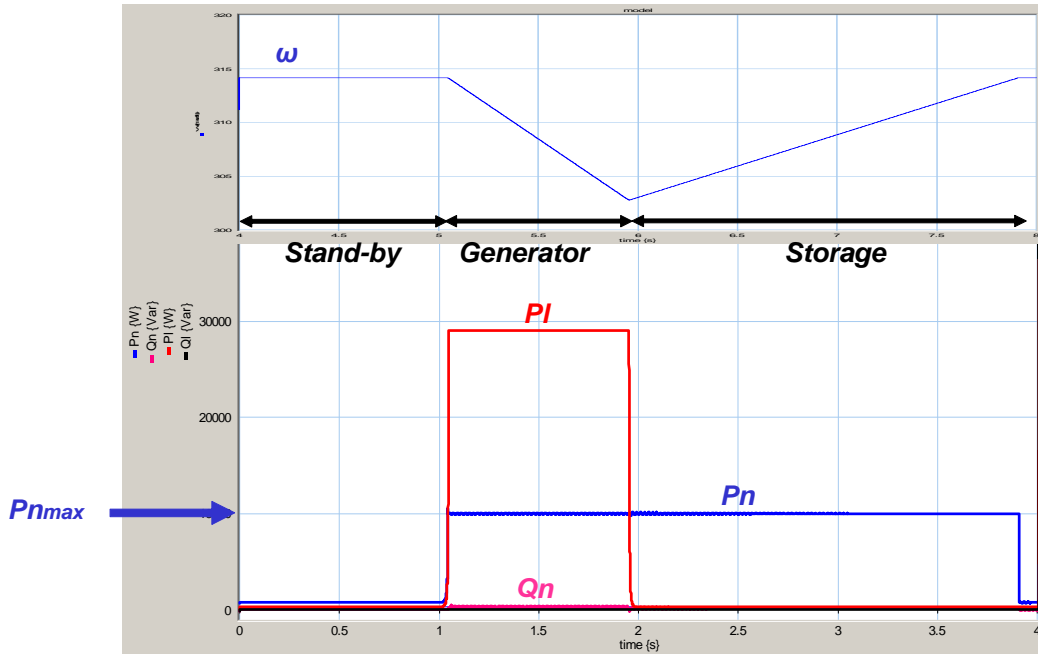
Figure 3: Active load and network powers (below) and mechanical speed for a varying resistive load.
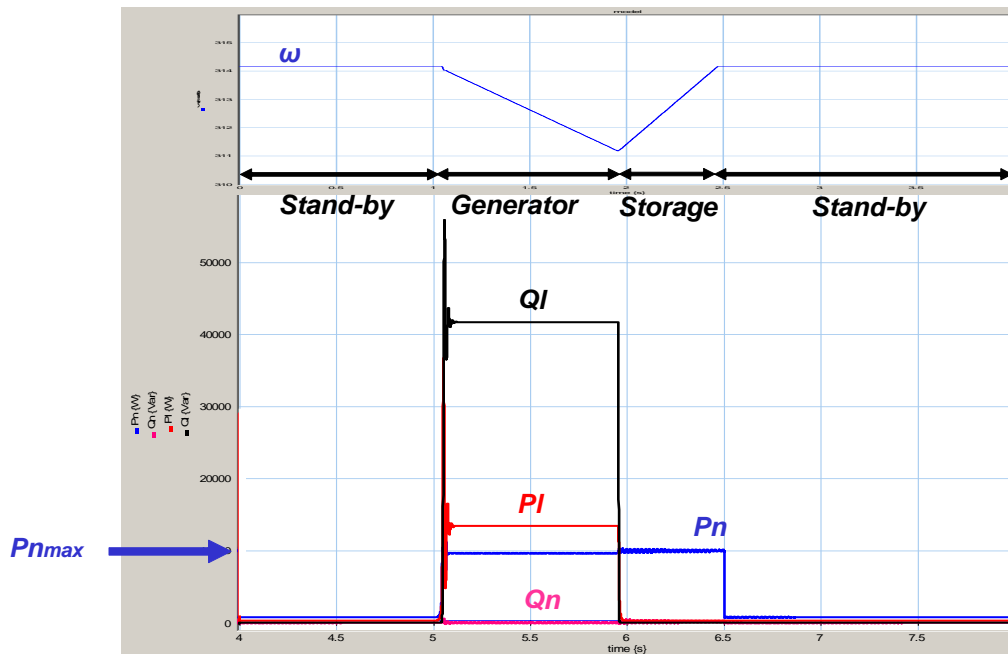

Figure 4: Active and reactive load and network powers (below) and mechanical speed for a varying resistive-inductive load.

8   Conclusions

IDA–PBC techniques have been applied to the control of a doubly-fed induction machine in order to manage the power flow between a mechanical source (flywheel) and a varying local load, under limited grid power conditions. We have been able to solve the IDA–PBC equations by assigning the desired Hamiltonian and introducing a variable damping to eliminate the resulting singularity. The controller obtained is globally stable and decouples the mechanical and electrical subsystems in the interconnection matrix. An indirect adaptive scheme has also been introduced to estimate the machine resistances.

The system not only provides the active power required by the load, but at the same time compensates the reactive power, so that the power grid sees the load+machine system as a pure resistive load, even for varying inductive local loads. There is no actual restriction about the kind of local load, as long as its parameters allow the assignment of equilibrium points.

Currently we are working on the experimental validation of the proposed controller, the implementation of the controller through a power converter connected also to the grid and the introduction of a grid model instead of the ideal bus considered in this paper.

References

[1] *20sim* modeling and simulation software, see: `www.20sim.com`.

[2] Akagi, H., and H. Sato, Control and performance of a doubly-fed induction machine intended for a flywheel energy storage system, *IEEE Transactions on Power Electronics* **17**, pp. 109-116, 2002.

[3] Caratozzolo, P., *Nonlinear control strategies of an isolated motion system with a double-fed induction generator*, PhD Thesis, Universitat Politècnica de Catalunya, 2003.

[4] Dalsmo, M., and A. van der Schaft, On representations and integrability of mathematical structures in energy-conserving physical systems, *SIAM J. Control Optim.* **37**, pp. 54-91, 1998.

[5] Fujimoto, K., and T. Sugie, Canonical transformations and stabilization of generalized Hamiltonian systems, *Systems & Control Letters*, Vol. 42, No. 3, pp. 217–227, 2001.

[6] Krause, Paul C., *Analysis of electric machinery*, McGraw-Hill, 1986.

[7] Krause, Paul C., and Oleg Wasynczuk, *Electromechanical motion devices*, McGraw-Hill, 1989.

[8] Kugi, A., *Non-linear control based on physical models*, Springer, 2001.

[9] Leonhard, W., *Control of electric drives*, Springer, 1995.

[10] Ortega, R., A. Loria, P.J. Nicklasson, and H. Sira-Ramirez, *Passivity-based control of Euler-Lagrange systems*, Communications and Control Engineering, Berlin, Germany, Spring-Verlag, 1998.

[11] Ortega, R, A. van der Schaft, B. Maschke and G. Escobar, Interconnection and damping assignment passivity-based control of port-controlled Hamiltonian systems, *Automatica* **38**, pp. 585-596, 2002.

[12] Panteley, E., R. Ortega, and P. Moya, Overcoming the detectability obstacle in certainty equivalence adaptive control, *Automatica* **38**, pp. 1125-1132, 2002.

[13] Peña, R., J. C. Clare and G. M. Asher, Doubly fed induction generator using back-to-back PWM converters and its application to variable speed wind-energy generation, *IEE Proc. Electric Power Applications*, **143**, pp. 231-241, 1996.

[14] Peña, R., J. C. Clare and G. M. Asher, A doubly fed induction generator using back-to-back PWM converters supplying an isolated load from a variable speed wind turbine, *IEE Proc. Electric Power Applications*, **143**, pp. 380-387, 1996.

[15] Rodríguez, H., and R. Ortega, Stabilization of electromechanical systems via interconnection and damping assignment, SUPELEC preprint, may 2002.

[16] Slootweg, J.G., H. Polinder, and W.L. Kling, Dynamic modelling of a wind turbine with doubly fed induction generator, IEEE Power Engineering Society Summer Meeting 2001, pp. 644-649, 2001.

[17] Sontag, E. D., On stability of perturbed asymptotically stable systems, *IEEE Trans. Automat. Contr.*, Vol. 48, No. 2, Feb. 2003, pp. 313–314.

[18] Peresada, S., A. Tilli and A. Tonielli, Robust output feedback control of a doubly-fed induction machine, Proceedings of the 25th Annual Conference of the IEEE Industrial Electronics Society (IECON '99), pp. 1348-1354, 1999.

[19] Peresada, S., A. Tilli and A. Tonielli, Power control of a doubly fed induction machine via output feedback, *Control Engineering Practice*, **12**, pp. 41-57, 2004.

[20] van der Schaft, A., L_2 *gain and passivity techniques in nonlinear control*, 2nd Edition, Springer, 2000.

A   Appendix A

Lemma 1 *Let us consider a system of the form*

$$
\begin{aligned}
\dot{x}_1 &= f_1(x_1, x_2), \\
\dot{x}_2 &= -Bx_2 + h(x_1),
\end{aligned}
\tag{23}
$$

where $x_1 \in \mathbb{R}^n$, $x_2 \in \mathbb{R}$, $B > 0$ and h is a continuous function. Assume that the system has fixed points x_1^*, x_2^*, and $\lim_{t \to +\infty} x_1(t) = x_1^*$ for any $x_2(t)$. Then $\lim_{t \to +\infty} x_2(t) = x_2^*$.

Proof.. Let $(\sigma_1(t), \sigma_2(t))$ be a given solution to (23). Since $\lim_{t \to +\infty} \sigma_1(t) = x_1^*$ it follows that $\sigma_1(t)$ is bounded and so is $h(\sigma_1(t))$. Since $Bx_2^* = h(x_1^*)$, it follows that $\forall \epsilon > 0\ \exists T > 0$, which may depend on $\sigma_1(t)$ and $\sigma_2(t)$, such that if $t > T$ then $|h(\sigma_1(t)) - Bx_2^*| < \epsilon \frac{B}{2}$. Using

$$
1 = e^{-Bt} + B \int_0^t e^{-B(t-\tau)} \mathrm{d}\tau
$$

it is immediate to write,

$$\sigma_2(t) - x_2^* = e^{-Bt}(x_2(0) - x_2^*) + \int_0^t e^{-B(t-\tau)}(h(\sigma_1(\tau)) - Bx_2^*)\mathrm{d}\tau$$

$$= e^{-Bt}(x_2(0) - x_2^*) + \int_0^T e^{-B(t-\tau)}(h(\sigma_1(\tau)) - Bx_2^*)\mathrm{d}\tau$$

$$+ \int_T^t e^{-B(t-\tau)}(h(\sigma_1(\tau)) - Bx_2^*)\mathrm{d}\tau$$

where $t > T$ has been assumed. There exists $\tilde{T} > 0$ such that if $t > \tilde{T}$ then

$$e^{-Bt}\left(x_2(0) - x_2^* + \int_0^T e^{B\tau}(h(\sigma_1(\tau)) - Bx_2^*)\mathrm{d}\tau\right) < \frac{\epsilon}{2},$$

where the boundedness of h has been used. Furthermore

$$\left|\int_T^t e^{-B(t-\tau)}(h(\sigma_1(\tau)) - Bx_2^*)\mathrm{d}\tau\right| < \int_T^t e^{-B(t-\tau)}\epsilon\frac{B}{2}\mathrm{d}\tau = \frac{\epsilon}{2}(1 - e^{-B(t-T)}) < \frac{\epsilon}{2}.$$

Finally, taking $t > \max\{T, \tilde{T}\}$, one gets $|\sigma_2(t) - x_2^*| < \epsilon$. This ends the proof. ◁